2008 IEEE/RSJ International Conference on Intelligent Robots and Systems
Acropolis Convention Center
Nice, France, Sept, 22-26, 2008

Modeling of Conditions where a Puncture Occurs during Needle Insertion considering Probability Distribution

Yo Kobayashi, Akinori Onishi, Takeharu Hoshi, Kazuya Kawamura,
and Masakatsu G. Fujie, *Members, IEEE*

***Abstract* - Needle insertion treatments require accurate placement of the needle tip into the target cancer. However, it is difficult to insert the needle into the cancer because of cancer displacement due to the organ deformation. Then, a path planning using numerical simulation to analyze the deformation of the organ and the timing of puncture is important for the accurate needle insertion. In this study, we have explained the modeling of conditions where the puncture occurs. Firstly, this paper shows needle insertion experiments for the hog liver in order to measure the needle force and displacement where the puncture occurs. According to the experimental results, significant variations in puncture force were observed. Accordingly, we proposed a novel condition of the force causing a puncture considering probability distribution. We summarized variations of the puncture force in the experimental data and represented conditions where a puncture occurs with probability distribution models where the force is random variable. In addition, the boundary conditions and liver shapes are considered by analyzing the stress status near the needle. Then, we derived the conditions of the puncture with probability distribution models where the stress is random variable.**

I. Introduction

A. Percutaneous therapy and robot-assisted needle insertion

One of the most common procedures employed in clinical practice is needle insertion. Recently, needle insertion, such as radiofrequency ablation (RFA) and percutaneous ethanol injection therapy (PEIT), have been used for cancer therapy. Since these treatments are based on minimally invasive surgery and achieve positive results, future applications are likely to be widespread, to cover the entire range of bodily organs. Recently, there has been a need for early diagnosis and treatment. With this in mind, accurate needle insertion will be important as one of the localized forms of treatment for small cancers diagnosed early.

In recent years, research and development has been carried out into surgical robots and navigation systems for minimally invasive and precise surgery [1]. Research into robotic systems to assist needle insertion has also been conducted; aiming to improve the needle placement accuracy and the expansion of the approach path. The authors are also engaging in research to develop robot assisted surgery systems based on the physical organ model shown in Fig. 1 [2]-[7].

B. Planning for needle insertion treatment

Needle insertion treatments require accurate placement of the needle tip into the target cancer. However, it is difficult to insert the needle toward the target cancer because of organ deformation. The needle insertion site, for example, in the case of the liver, is very soft, and it is easy for the force of the needle to deform the tissues, meaning the position of the target cancer will also be displaced. Then, the needle insertion from a certain path is required so that the tip of the needle can be delivered correctly in the target cancer. In this case, the needle must direct the center of target lesion when the puncture occurs to ensure accurate placement into the cancer, since the needle advances inside the tissue when puncturing the liver. Therefore, a plan for the insertion path must be devised; taking liver deformation into account.

For the above planning method, a numerical simulation in a virtual surgery environment, reproduced with physical deformable models of organs, may be used. Especially, it is important to conduct an accurate simulation of organ deformation with appropriate conditions when a puncture occurs for the above reasons.

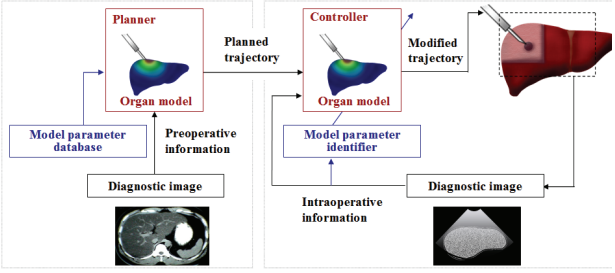

Fig. 1 The needle insertion system based on the physical organ model

Manuscript received February 22, 2008. This work was supported in part by the 21st Century Center of Excellence (COE) Program "Innovative research on symbiosis technologies for humans and robots in an elderly dominated society", Waseda University, Tokyo, Japan, and partly by the "Establishment of a Consolidated Research Institute for Advanced Science and Medical Care", Encouraging the Development Strategic Research Centers Program, Special Coordination Funds for Promoting Science and Technology, Ministry of Education, Culture, Sports, Science and Technology, Japan and partly by "the robotic medical technology cluster in Gifu prefecture," Knowledge Cluster Initiative, Ministry of Education, Culture, Sports, Science and Technology, Japan. This research was partially supported by the Ministry of Education, Science, Sports and Culture, Grant-in-Aid for 2008, 19-53203.

Y. Kobayashi are Consolidated Research Institute for Advanced Science and Medical Care, Waseda University, Japan, (59-309, 3-4-1, Ohkubo Shinjuku-ku, Tokyo, Japan, phone: +81-3-5286-3412; fax: +81-3-5291 -8269; e-mail: you-k@aoni.waseda.jp).

A. Onishi, T. Hoshi and K. Kawamura are with the Graduate School of Science and Engineering, Waseda University, Japan.

M. G. Fujie is with the Graduate School of Science and Engineering, Waseda University, and the Faculty of Science and Engineering, Waseda University, Japan.

A number of research groups are conducting studies on planning for needle insertion using a finite element method (FEM). For example, Alterovitz et al. have researched the numerical simulation of steerable needle insertion for prostate branch therapy [9]-[10]. Meanwhile, DiMaio et al. have developed a linear system for measuring the extent of planar tissue phantom deformation during needle insertion, using a linear elastic material model [11]-[12]. Salcudean et al. shows the planning system to determined the optimized insertion angle and position using a linear and nonlinear organ model, while Alterovitz et al. present a planning system for steerable needle insertion for brachytherapy cancer treatment [13]-[14].

At the same time, many research groups research details of measurement concerning the relation between the needle displacement and force during needle insertion using animal organs and investigate conditions where puncture occurs. For example, Okamura et al. have developed empirical models for the needle insertion force, comprising tissue stiffness force, friction force, and puncture force [15]-[18], while Heverly et al. show the velocity dependency of the puncture force of biomaterial [19].

It is well known and related works[15]-[19] have reported that the time of the puncture varies for each experiment, and even under identical conditions, inconsistency of force and needle displacement can be observed. This experimental data suggests that consideration of the potential variance in puncture conditions is required in order to set approximate conditions for the puncture. However, related research into the conditions of the puncture is based upon the fixing value of the needle force in related work, while the probability consideration associated with the condition of the puncture has not yet been fully researched.

C. Objectives

It is vital to evaluate these properties concerning the variation in the time of the puncture and be properly set up the condition when the puncture occurs in the needle insertion simulation. Then, the purpose of this study is the detailed modeling of conditions where a puncture occurs. The originality of this report is as follows:

Conditions where puncture occurs with consideration of probability distribution: the variance of experimental data even under identical conditions means it is difficult to deterministically specify the puncture conditions. In this study, we summarized variations of the puncture force in the experimental data and represent the conditions where punctures occur via probability distribution models.

This report consists of the following sections:

- Section II shows the needle insertion experiment conducted on the hog liver to measure the force exerted on the needle and the needle displacement when the puncture occurs and summarizes the variation in the experiment data.
- Section III shows the modeling concerning the conditions of force where the puncture occurs; with probability consideration based on the variances of the experimental result obtained in section II.
- Section IV shows consideration about the boundary conditions and liver shapes by analyzing the stress status near the needle. The modeling of stress conditions where a puncture occurs, with probability consideration from the analysis using the physical liver model.

II. Needle Insertion Experiment

This section shows the needle insertion experiment on the hog liver; used to measure the force applied to the needle and the needle displacement when the puncture occurs, in order to investigate the conditions under which the puncture occurs. At this time, several needle insertion experiments performed under identical conditions are necessary so that the variation of experiment data can be obtained. Moreover, we investigate the velocity dependency of the force applied to the needle and the needle displacement itself when the puncture occurs, because it is well known and related works [19] have reported that the timing of the puncture is dependent on the needle velocity.

A. Methods

Details of the experimental setup are shown as follows; as well as an overview of the measurement experiment in Fig. 2.

I) Liver shape/boundary condition: The liver was cut in a rectangular shape (50 x 50mm, thickness approx. 20mm) and was placed on the measurement table. The dorsal aspect of the liver is fixed by the wall. When the liver was fixed, double sided tape was used to place sandpaper on the wall, whereupon the liver and sandpaper were attached to each other with instant glue.

II) Experimental equipment: The needles used in this study were those used for biopsy (17 gauges). As shown in Fig. 2, configuration of the experimental equipment is performed by a linear actuator with force sensor (BL AUTOTECH: BL NANO).

III) Experimental conditions: The experiments were carried out with the needle insertion velocity ranging from 0.5mm to 8mm/s, while the experimental conditions of the needle insertion velocity were set to 7 patterns (0.5, 1.0, 2.0, 3.0, 4.0, 6.0, and 8.0) in order to perform 9 trial experiments for each velocity (total 63 trials). The experiments were conducted with 3 parts of the liver removed from a single hog, while the force loaded on the needle and the needle displacement were measured during each experiment.

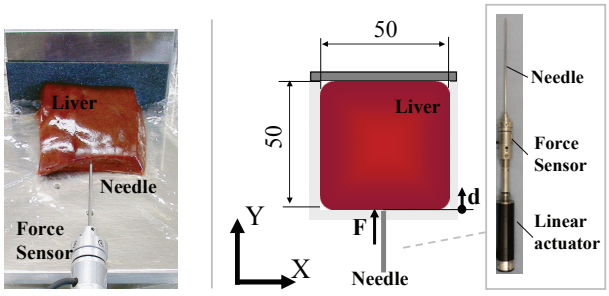

Fig. 2 Experimental conditions and experimental equipment

B. Results

Figure 3 shows the relation between the needle displacement and the force applied to the needle during the experiment. The data in Fig. 3 shows an example when the needle insertion velocity is 4 mm/s. As shown in previous work [16], the main puncture is designated by the force peaking after a steady rise, followed by a sharp decrease. This data explains that when the needle punctures the liver it does not keep cutting the tissue with consistent force. Instead, 1) it pushes the tissue and 2) the tissue is subsequently punctured instantaneously (Fig. 3).

The purpose of this study is the modeling of 2), namely the condition whereby the puncture instantaneously occurs. Below, the force applied to the needle where the puncture occurs is defined as the puncture force F_c while the displacement at the puncture is defined as the puncture displacement d_c.

For each piece of data, the puncture displacement and puncture force were manually extracted in order to summarize each needle insertion velocity. Figs. 4 and 5 show the data of puncture force for each needle insertion velocity and the data of puncture displacement for each needle insertion velocity, respectively. In both Figs. 4 and 5, the blue plots represent experimental data, while the red plots represent the median of each needle insertion velocity.

C. Discussions

a) Considerations on the variation of the experiment results: According to Figs. 4 and 5, significant variations are observable in both the puncture force and puncture displacement. Even when the needle insertion experiments are conducted under virtually identical conditions, variations emerge in both the results of the puncture force and puncture displacement. Therefore, it is considered that the conditions under which the puncture occurs can be determined by the micro status of the needle and the tissue. With this in mind, it is very difficult to precisely reproduce these micro statuses on the simulator and deterministically set the conditions where a puncture occurs.

In case the condition where a puncture occurs is set deterministically and no consideration is made in terms of variations of the puncture by the needle insertion simulator, the actual phenomena may not be precisely reproduced in many cases. Therefore, it is necessary to consider variations when the puncture conditions are modeled, and thus significant to probabilistically consider the conditions where puncture occurs.

b) Specifying parameters which cause puncture phenomenon: Since organs such as the liver have viscoelasticity[2]-[3], the relation between the stress and strain of the tissue cannot be uniquely determined but varies depending on the needle insertion velocity. Therefore, it is vital to specify which parameter (either stress or strain) contributes to the puncture phenomenon. Here, we assume that the puncture occurs due to either parameter (stress or strain); using the experimental results to model the puncture conditions.

Subsequently, the consideration was advanced using the median values shown in Figs. 4 and 5. The median values of puncture force indicated in Fig. 4 show that the puncture force has no velocity dependency but shows virtually constant values. On the other hand, the median values of puncture displacement shown in Fig. 5 show how the puncture displacement decrease as the needle insertion velocity rises.

The stress status of the tissue near the needle tip is proportional to the force applied to the needle and the strain status is proportional to the needle displacement. Since the puncture displacement has velocity dependency, the strain state of tissues near the needle when the puncture occurs varies depending on the needle insertion velocity. Therefore, it is considered inappropriate to set conditions using the strain size near the needle. On the other hand, stress values near the needle when the puncture occurs remain constant; regardless of the needle insertion velocity. This suggests that the puncture occurs when the stress near the needle becomes constant, and it is considered appropriate to set puncture conditions by using the stress size of the tissue near the needle.

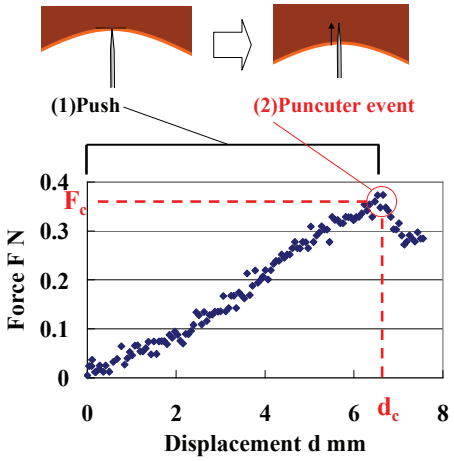

Fig. 3 Relation between the needle displacement and force (needle insertion velocity: 4 mm/s) and events in needle insertion [16]

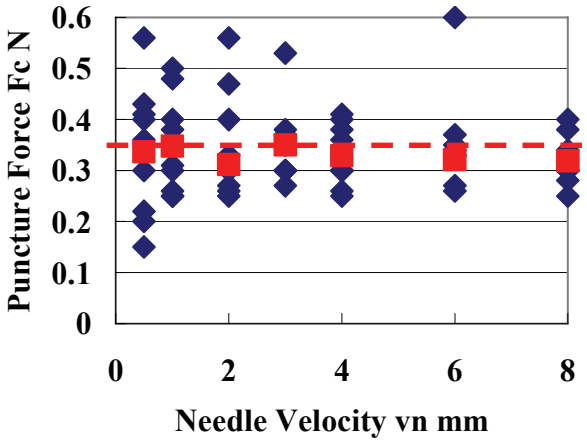

Fig. 4 Relation between the needle insertion velocity and the puncture force F_c

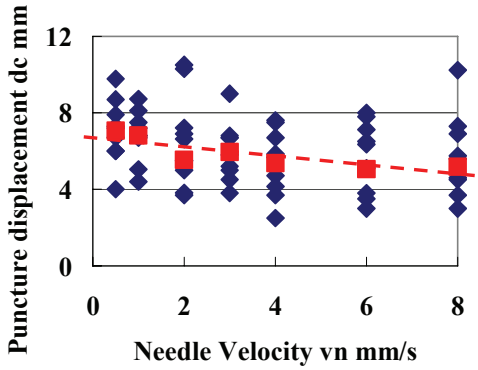

Fig. 5 Relation between the needle insertion velocity and the puncture displacement d_c

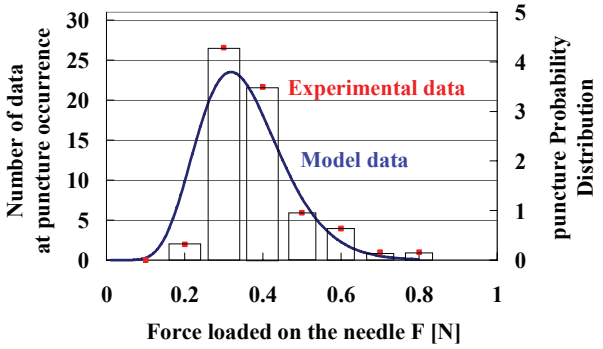

Fig. 6 Probability distribution model. The Y axis on the left side represents the number of samples existing in the interval, while the Y axis on the right side represents the discrete probability distribution.

Based on these considerations of a) and b), it was confirmed that probabilistic consideration is necessary to assess variations of the experimental data and evaluation of stress status near the needle is also necessary.

The following section III explains consideration of the probability of the force causing a puncture and the modeling of the same. In addition, section IV shows analysis of the stress status near the needle tip considering the boundary conditions and liver shapes; using the physical model of the liver and reproducing the experimental conditions in the experiment of this section.

III. Probability Model of the Force When a Puncture Occurs

In this section, a model showing the probability of puncture occurrence when a certain needle insertion force is applied to the liver is derived from evaluating variations of puncture forces.

The probability of puncture occurrence at the time when a certain needle insertion force is applied to the organ is defined as "Puncture probability distribution p". Likewise, the probability of a puncture phenomenon already occurring when a certain needle insertion force is assumed is defined as "puncture probability P". Based on the above definitions, the following discussion shall ensue.

A. Histogram

A histogram of the data obtained in section II was created to visualize the status of distribution of the puncture force F_c and a histogram hierarchy was calculated from a total of 63 data by using the Sturges' formula to be determined in 7. The histogram of the puncture force F_c is shown in Fig. 6. Here, the Y axis on the left side of Fig. 6 represents the number of samples existing in the interval, while the Y axis on the right side of Fig. 6 represents the discrete probability distribution, where this latter value was calculated using (1):

$$f_i(i) = \frac{n_i}{N\lambda_i} \tag{1}$$

Here, n_i, λi and N represent the number of data for the i interval, space of the i interval and the number of total data, respectively.

B. Puncture probability distribution model

The puncture probability distribution p is modeled from the histogram shape of the puncture force created in section III(A). The shape of the histogram of puncture force shows the following features:

- The force required for puncture is defined only in the non-negative region.
- A histogram in Fig. 6 shows a distorted distribution; centering on around 0.35[N].

With the above features in mind, the gamma distribution shown in (2) was employed as a model representing puncture probability distribution p:

$$p(F) = \frac{F^{\alpha-1}}{\beta^{\alpha}\Gamma(\alpha)}\exp\left(-\frac{F}{\beta}\right) \tag{2}$$

Here, F is the force applied to the needle, while α and β are parameters to determine the shape of the gamma distribution, and Γ() is the gamma function. In gamma distribution, the relation of parameters α and β, median μ and variance s is as shown below:

$$\mu = \alpha\beta \tag{3}$$

$$s^2 = \alpha\beta^2 \tag{4}$$

Figure 6 also shows the probability distribution modeled by gamma distribution. The values of parameters α and β in Table I were determined by using the relation of (3)-(4) from the values of the median μ and variance s; calculated by a total of 63 data as shown in Fig. 4.

Figure 6 shows that the histogram showing the status of puncture force distribution and the puncture probability distribution model with gamma distribution indicate similar tendencies. This result confirmed it is possible for the gamma distribution to model the puncture probability distribution; representing a variation of experimental data.

TABLE I PARAMETERS OF (2)-(4)

u	s	α	β
0.35	0.34	10	0.34

C. Puncture probability model

The relation between the puncture probability distribution p and the puncture probability P is shown as (5); based on the relation between the probability density function and the probability:

$$P(F) = \int_0^F p(x)\,dx \tag{5}$$

According to formula (5), the puncture probability P is calculated by integrating the puncture probability distribution p, shown in (2), to the force F loaded on the needle.

Using (5), the puncture probability P for each force F loaded onto the needle was calculated by the puncture probability model shown in (2). The calculation result is shown in Fig. 7, while the histogram of the puncture probability calculated from the experiment result in Fig. 4 is also shown in Fig. 7. The discrete probability was calculated by using (6).

$$P(i) = \sum_{j=1}^{i} \frac{n_i}{N} \tag{6}$$

Looking at Fig. 7, it shows that the histogram showing the puncture probability from experimental data and the puncture probability as calculated by the puncture probability model indicate similar tendencies. Based on this result, it was confirmed that the puncture probability P can also be precisely modeled using the proposed probability model.

IV. Consideration of Stress Near the Needle Tip

The relation between the force applied to the liver and the displacement varies depending on the boundary conditions and liver shapes. For this reason, the puncture probability distribution model shown with (2) cannot be used as the same parameter when the boundary conditions and liver shapes differ. In order to conduct a setup of conditions that do not depend on the boundary conditions and liver shapes, it is necessary to represent the puncture probability distribution model by the stress status near the needle.

In this section, the physical models of the liver were developed under conditions identical to the experiment shown in section II in order to estimate the stress status near the needle. Using the results, we discussed the puncture probability distribution model where the stress is random variable.

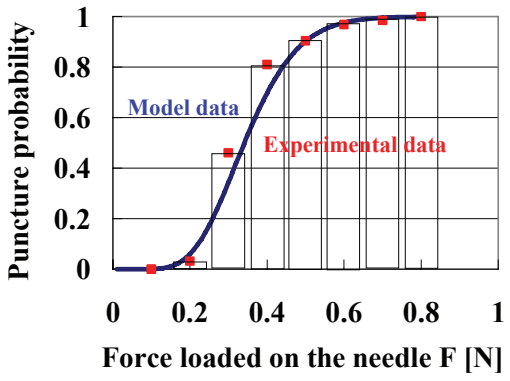

Fig. 7 Puncture probability model

A. Methods

The author et al. have studied about the physical model of the liver, taking viscoelasticity and nonlinearity into consideration [2]-[3], and reported on methods to establish a deformable model of the liver using Finite Element Method (FEM) [4]-[5] as well as an validation experiments for the same [6]. This liver model can analyze the deformation and stress-strain state of each part of the liver during the needle insertion. It is assumed from the validation experiments [6] that the liver model reproduces nonlinear and viscoelastic responses equivalent to a real liver, including the velocity dependency of a puncture phenomenon.

In this paper, a numerical simulation with a physical model of the liver is used to obtain stress data during the needle insertion. This numerical simulator is necessary to analyze the stress value because few means exist to measure the stress values of the liver directly.

When conducting analysis using the FEM, results may vary depending on the mesh shape. In particular, it is known that the mesh needs to be set small, especially for the precise analysis of stress and so on, in the area where the boundary conditions rapidly change. The contact point between the needle and liver corresponds to the area where the boundary conditions rapidly change, and here, the stress status of the tissue near the needle is considered to be significantly dependent on the size of the mesh.

Therefore, we prepare a liver model with a different-sized mesh near the contact point in order to compare those analysis results. According to the result, the effect of the mesh shape on the stress status near the contact point is discussed.

The liver models and the details of the simulation conditions are shown below. In the following analysis, we used the physical liver models with considerations of the viscoelasticity and linearity proposed in our previous works [4]-[6].

1) Setting the boundary condition of the liver model: A model with a shape similar to the liver used in the experiment of section II was developed. The shape of the liver model was a 50 x 50mm rectangle and the thickness was also 20mm, the same as the liver used in the experiment. As boundary conditions, the dorsal side of the model was set as the fixed end. The model shape and the boundary conditions are shown in Fig. 8.

2) Setting the mesh: The mesh was developed using the Delaunay method, which involves dividing the object automatically into triangular elements, based on the outline of the target object. It is one of the most accepted methods with uniquely high reliability due to its geometric division. The mesh (a) was created to form a circumscribed circle diameter of 5mm for the entire triangle. Based on the mesh (a), other meshes (b)-(h) were created by changing the circumscribed circle of the elements existing within a radius of 20mm from the point where the needle makes contact. Table II shows the size of the circumscribed circle of the element near the needle of each mesh (a)-(h), while Fig. 8 also shows meshes (a) and (d), and each of the model shapes.

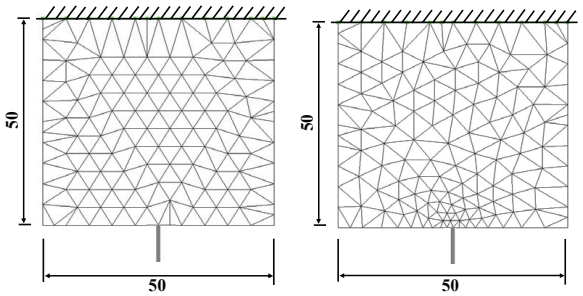

Fig. 8 Boundary condition of the liver model and produced mesh (a),(d)

TABLE II MESH SIZE OF THE ELEMENT NEAR THE NEEDLE

Type	(a)	(b)	(c)	(d)	(e)	(f)	(g)	(h)
size mm	5.0	2.5	1.77	1.25	0.88	0.63	0.44	0.32

3) Simulation conditions: A node at needle contact was forced to displace towards the Y axis to 10mm at 4mm/s when the simulation was performed. Each stiffness parameter of the liver model was manually set to correspond with the behavior of the experimental results in Fig. 3. The simulation results using mesh (a) were referred to when the parameters of the liver model were set.

4) Stress on the tissue near the needle: As a element to represent the tissue near the needle, an element existing in the direction in which the needle axis is directed is used (Fig. 9). The stress of that element is defined as that of the tissue near the needle, the value of that is considered to alter the probability of puncture occurrence.

B. Model of puncture probability distribution

In this section, we explain the deriving of the puncture probability distribution model where the stress is random variable. The simulation using the liver model of mesh (a) is used to discuss following modeling of puncture condition.

Figure 10 shows the simulation results when the mesh (a) is used. The color of each element implies the stress in Fig. 10. As a result of the simulation using the liver model, the force applied to the liver and the stress near the needle are almost proportional, which can be represented with (7). The Mises stress is used to evaluate the extent of the stress.

$$\sigma = \kappa F \tag{7}$$

Here, κ is a proportional constant to relate the force applied to the needle and the stress near the needle. The value of κ is about 13700 in the case of the simulation using mesh (a).

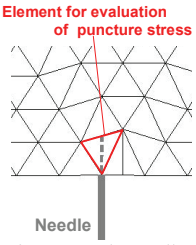

Fig. 9 Definition of the tissue near the needle

By assigning (7) to (2), the puncture probability distribution model using the stress status near the needle is presented with (8).

$$f(\sigma) = \frac{\sigma^{\alpha'-1}}{\beta'^{\alpha'}\Gamma(\alpha')}\exp\left(-\frac{\sigma}{\beta'}\right) \tag{8}$$

Here, σ is the stress status near the needle and α' and β' are parameters used to determine the shape of the gamma distribution, which has the following relations with α and β of the formula (9)-(10):

$$\alpha' = \alpha \tag{9}$$

$$\beta' = \beta / \kappa \tag{10}$$

From (3)-(4), the median μ' and variance s' are also as below:

$$\mu' = \mu / \kappa \tag{11}$$

$$s'^2 = \left(s / \kappa\right)^2 \tag{12}$$

The values of parameters α' and β' in Table III were determined by using the relation of (9)-(12) from the values of κ.

Figure 11 shows a model of the puncture probability distribution where the stress value is random variance. This probability distribution model can be used to determine the puncture conditions of liver models, regardless of the boundary conditions and liver shapes.

C. Dependence on the mesh

Consideration of the mesh size near the needle will be described in this section. Figure 12 shows the analysis results when the mesh (d) was used. In Fig. 12, the color of each element implies the stress. Compared with the analysis results of mesh (a) shown in Fig. 10, it is apparent that the stress value near the needle is greater in the analysis results of mesh (d).

In each mesh (a)-(h), the parameters of a puncture probability distribution model and the median of puncture stress σ_c were calculated. Figure 13 summarizes the relation between the size of each mesh (a)-(h) and the median of puncture stress σ_c. According to the results in Fig. 13, the relation between the mesh size and the median of puncture stress σ_c, increases almost linearly on both logarithmic axes, which can be precisely approximated by using the formula (13):

$$\sigma_c(\delta) = a\delta^{-b} \tag{13}$$

Here, δ is the circumscribed circle diameter of the mesh near the needle (mesh size), while a, b are parameters which can be determined by the straight line slope and the intercept.

As shown in the A3) simulation setup, the effects of the needle on the liver model of this analysis are represented with the enforced displacement to a contact node. This implies that

TABLE III PARAMETERS OF (8)-(12)

u'	s'	α'	β'
4800	1500	10	470

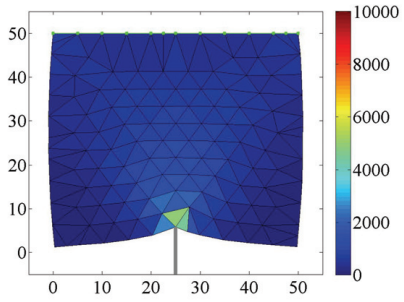

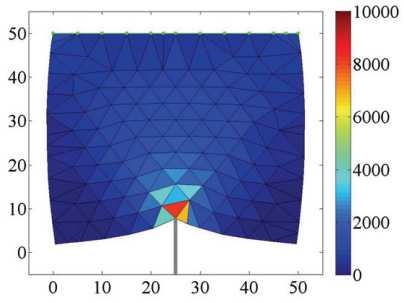

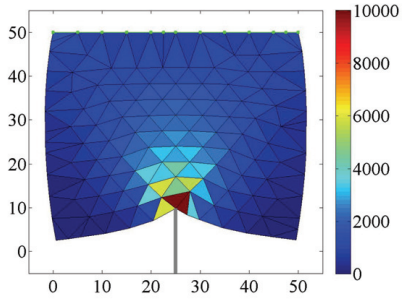

Fig. 10 Deformation results of the liver model (mesh a)

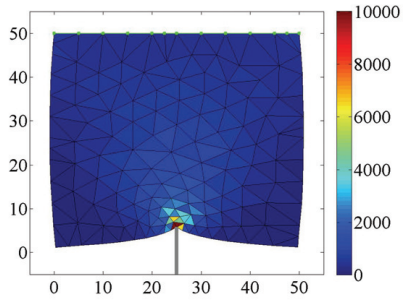

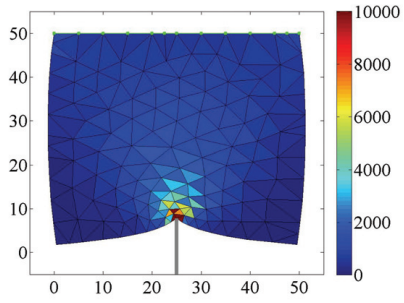

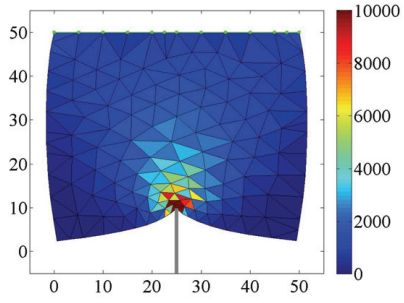

Fig. 12 Deformation results of the liver model (mesh d)

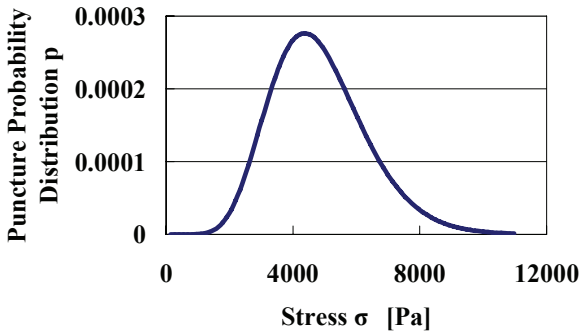

Fig. 11 Histogram and puncture probability distribution model

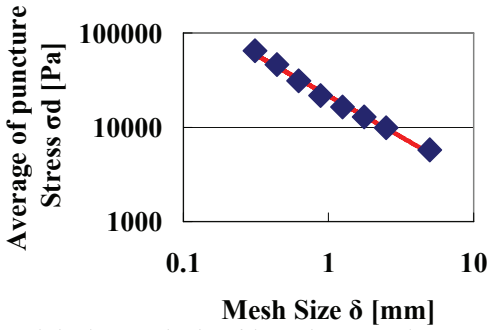

Fig. 13 Relation between the size of the mesh screen and stress σ_c on the tissue near the needle

the force applied to the liver by the needle is defined as a concentrated force (a single point of maximum weight). For this reason, it is suggested that the stress increases as the setting of the mesh size becomes smaller.

It is possible to obtain detailed knowledge concerning the stress near the needle by conducting stress analysis with a setting featuring a mesh of sufficiently small size for a needle diameter of 1.5mm. However, in this case, the needle contact status for the small mesh of the organ must be described in detail, which brings other substantial problems, such as cumbersome settings and a potentially vast increase in the calculation time required.

Therefore, in this study, we propose a method to change the stress condition where puncture occurs in response to the size of the mesh. It means that each parameter (α' and β') of the probability distribution model (8) is modified corresponding to the mesh size.

According to the simulation result shown in the formula (13), each parameter of the probability distribution model (8) is shown with the formula (14)-(15) when the mesh size of the tissue near the needle is δ.

$$\alpha' = \alpha \tag{14}$$

$$\beta' = \frac{c}{a\delta^{-b}} \tag{15}$$

In line with the mesh size of the model, setting each parameter by using formulas (14) and (15) enables us to appropriately set the probability distribution of the puncture stress on simulations.

TABLE IV PARAMETERS OF (13)-(15)

a	b	c	α'
22000	0.87	2500000	10

V. CONCLUSIONS AND FUTURE WORK

In this paper, we explained the modeling of conditions where a puncture occurs, in order to develop a planning system for needle insertion. Firstly, this paper shows needle insertion experiments for the liver to measure the force applied to the needle and the needle displacement where the puncture occurs. Based on these results, we summarized the velocity dependency of the displacement where the puncture occurs and assumed that the conditions whereby the liver is punctured may be decided by the stress status of the tissue near the needle. Furthermore, we summarized variations of the puncture force in the experimental data in order to represent conditions where a puncture occurs with probability distribution models, where the force is random variable. In addition, the boundary conditions and liver shapes are considered by analyzing the stress status near the needle. Then, we derived the conditions of the puncture with probability distribution models where the stress is random variable. We also summarized the effects of the stress values according to the mesh size of the liver model. Based on these results, it became possible to appropriately set conditions where a puncture occurs on simulations.

From a future prospective, the proposed puncture condition model shall be confirmed using the data obtained in vivo. In addition, using a physical liver model and the puncture condition model proposed in this study, a study of the planning method used to determine the optimal insertion path to be made. A manipulator enabling high–accuracy positioning to realize needle placement at the insertion path shall be developed, while a robotic system, enabling accurate needle placement for liver cancer, can also be developed by integrating these technologies.

REFERENCES

[1] R. H. Taylor and D. Stoianovici "Medical Robotics in Computer-Integrated Surgery", IEEE Transactions on Robotics and Automation,Vol. 19, No. 5, pp.765-781,2003

[2] Y. Kobayashi, J. Okamoto, M. G. Fujie "Physical Properties of the Liver for Needle Insertion Control" , In IEEE International Conference on Intelligent Robotics and Systems (2004) , pp.2960-2966, 2004

[3] Y. Kobayashi, J. Okamoto, M.G. Fujie "Physical Properties of the Liver and the Development of an Intelligent Manipulator for Needle Insertion" , In IEEE International Conference on Robotics and Automation (2005), pp.1644-1651,2005

[4] Y. Kobayashi, A. Onishi, T. Hoshi, K. Kawamura and M. G. Fujie, "Viscoelastic and Nonlinear Organ Model for Control of Needle Insertion Manipulator", in Proceeding of the 29th Annual International Conference of the IEEE Engineering in Medicine and Biology Society, pp1242-1248, 2007

[5] Y. Kobayashi, A. Onishi, T. Hoshi, K. Kawamura and M. G. Fujie, "Deformation Simulation using a Viscoelastic and Nonlinear Organ Model for Control of a Needle Insertion Manipulator", in Proceedings of 2007 IEEE International Conference on Intelligent Robots and Systems, pp1801-1808, 2007

[6] Y. Kobayashi, A. Onishi, H. Watanabe, T. Hoshi, K. Kawamura and M. G. Fujie, "Experimental Validation of Viscoelastic and Nonlinear Model of Liver for Needle Insertion Simulation", in Proceedings of 2008 IEEE International Conference on Biomedical Robotics and Biomechatronics (accepted)

[7] T. Hoshi, Y. Kobayashi, K. Kawamura, M. G. Fujie, "Developing an Intraoperative Methodology Using the Finite Element Method and the Extended Kalman Filter to Identify the Material Parameters of an Organ Model", in Proceeding of the 29th International Conference of the IEEE Engineering in Medicine and Biology Society, pp.469-474, 2007

[8] D.Glozman, M. Shoham, "Image-Guided Robotic Flexible Needle Steering" , IEEE Transactions on Robotics and Automation, Volume: 23, Issue: 3, pp.459-467

[9] R.Alterovitz, A. Lim, K. Goldberg, G. S. Chirikjian, and A. M. Okamura, "Steering Flexible Needles under Markov Motion Uncertainty", In International Conference on Intelligent Robots and Systems (2005), pp120-125,2005

[10] R.Alterovitz, K. Goldberg, and A. Okamura, "Planning for Steerable Bevel-Tip Needle Insertion through 2D Soft Tissue with Obstacles", In IEEE International Conference on Robotics and Automation (2005), pp.1652-1657,2005

[11] S.P.DiMaio and S.E.Salcudean "Needle Insertion Modelling and Simulation", In IEEE Transaction on Robotics and automation ,Vol. 19, No. 5, pp864-875, 2003

[12] S.P.DiMaio and S.E.Salcudean "Interactive Simulation of Needle Insertion Model", In IEEE Transaction on Biomedical Engineering,Vol. 52, No. 7, pp.1167-1179, 2005

[13] O. Goksel , S.E. Salcudean, S. P. DiMaio, R. Rohling and J. Morris, "3D Needle-Tissue Interaction Simulation for Prostate Brachytherapy", in Medical Image Computing and Computer-Assisted Intervention (2005), pp.827-834, 2005

[14] E.Dehghan, S.E.Salcudean, "Needle Insertion Point and Orientation Optimization in Non-linear Tissue with Application to Brachytherapy", in 2007 IEEE International Conference on Robotics and Automation, pp.2267-2272, 2007

[15] H. Kataoka, T. Washio, M. Audette, and K. Mizuhara, "A Model for Relations between Needle Deflection, Force, and Thickness on Needle Penetration" , In Medical Image Computing and Computer Assisted Intervention (2001), pp.966-974,2001

[16] C.Simone and A.M.Okamura, "Modeling of Needle Insertion Forces for Robot-assisted Percutaneous Therapy" In IEEE International Conference on Robotics and Automation (2002), pp.2085-2091,2002

[17] M.D.O'Leary, T.Washio, K.Yoshinaka, and M.Okamura "Robotic Needle Insertion:Effects of Friction and Needle Geometry", In IEEE International Conference on Robotics and Automation (2003), pp.1774-1780,2003

[18] A.M.Okamura, C.Simone and M.D.O'Leary, "Force modeling for needle insertion into soft tissue", In IEEE Transaction on Biomedical Engineering,Vol. 51, No. 10, pp.1707-1716, 2004

[19] M.Heverly, P.Dupont, J.Triedman,"Trajectory Optimization for Dynamic Needle Insertion", In IEEE International Conference on Robotics and Automation (2005), pp.1646- 1651,2005